Numerical Simulation of Conductivity Changes in the Human Thorax Caused by Aortic Dissection

Alice Reinbacher-Köstinger, Vahid Badeli, Oszkár Bíró, and Christian Magele

Institute of Fundamentals and Theory in Electrical Engineering, Graz University of Technology, 8010 Graz, Austria

In case of an aortic dissection (AD), the aortic shape as well as the blood flow will be altered in the region concerned. Based on the thoracic electrical bioimpedance technique that allows to identify and quantify conductivity changes by measuring the impedance on the thorax, a numerical simulation model for investigating effects caused by ADs is proposed. In order to find a simple non-invasive method for the detection of ADs, the possibilities and limits of applying a bioimpedance technique are shown in this paper.

Index Terms—**Aortic dissection (AD), non-invasive measurement method, thoracic electrical bioimpedance (TEB).**

I. Introduction

AN AORTIC dissection (AD) is initiated by a small tear in the innermost layer of the aorta (intima), which leads to propagation of blood within the media layer as shown in Fig. 1. Depending on the location of the so-called false lumen, ADs are classified [1] as represented in Fig. 2. If the ascending aorta is involved (Stanford Type A), an acute condition with a high mortality rate within a few hours occurs in most cases due to the high blood pressure right after the aortic heart valve. On the other hand, Stanford Type B cases (in the descending aorta) may become chronic, which means that the onset of the dissection dates back more than 14 days and patients can be often treated with medical therapy. In both cases, the symptoms of AD patients are sudden severe chest or upper back pain, which are not clearly assignable to this disease. Thus, applying a non-invasive method to ascertain the presence of an AD is necessary.

Ultrasound scanning is a commonly used method that is fast and usually well-available, while magnetic resonance imaging has better resolution and, therefore, higher accuracy. Nevertheless, an easier to use and still reliable method for pre-identification of AD would be beneficial, since ultrasound scanning and magnetic resonance tomography are expensive and experts are needed to read and interpret the images.

The presence of a false lumen alters the aortic hemodynamics and also changes the tissue distribution in the thorax. Such changes can be basically identified and quantified by the thoracic electrical bioimpedance (TEB) technique. Two TEB techniques, which are already in clinical use, are the impedance cardiography (ICG) [3] and the electrical impedance tomography (EIT) [4] for measuring cardiodynamic parameters (e.g., the stroke volume and the cardiac output) and lung dysfunctions, respectively. EIT allows to identify the spatial conductivity distribution in the thoracic transverse plane, while ICG is focused on determining time-dependent conductivity changes. Since the spatial resolution of EIT is very coarse with respect to the cross section of the aorta, the method of ICG is basically used in this paper.

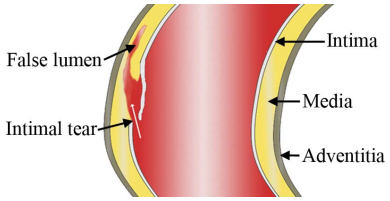

Fig. 1. Intimal tear in the aorta [2].

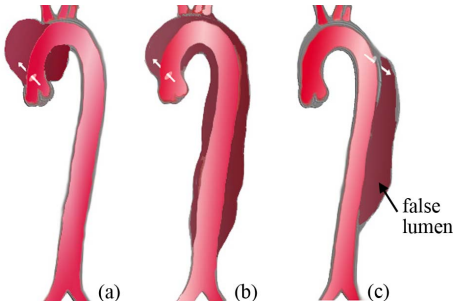

Fig. 2. Aortic dissection types. (a) and (b) Ascending aorta is involved (Stanford Type A). (c) Descending aorta is involved only (Stanford Type B) [2].

II. Methods

A. Thoracic Electrical Bioimpedance Technique

By injecting a low-amplitude alternating current into the human thorax and measuring the voltage drop between the two injection electrodes, the impedance of the thorax can be measured in principle. Since the conductivity of the blood-filled aorta is much higher compared to one of the surrounding tissue types as represented in Table I, changes of the measured impedance are strongly related to changes in the aorta.

During one cardiac pulse wave of about 1 s, the impedance decreases in the systolic phase (when the heart ventricles contract and thus force blood into the aorta) and increases in the diastolic phase (blood volume and flow in the aorta decreases). Studies have shown that there are two main reasons

Manuscript received November 4, 2018; revised January 4, 2019; accepted January 11, 2019. Corresponding author: A. Reinbacher-Köstinger (e-mail: alice.koestinger@tugraz.at).

Color versions of one or more of the figures in this paper are available online at http://ieeexplore.ieee.org.

Digital Object Identifier 10.1109/TMAG.2019.2895418

TABLE I
CONDUCTIVITY AND PERMITTIVITY OF THORACIC TISSUES [5]

Tissue type	σ in S/m	ε_r
Blood (stationary)	0.7	5120
Bone	0.02	228
Lung Deflated	0.27	5145
Lung Inflated	0.11	2581
Muscle	0.36	8089
Fat	0.02	93

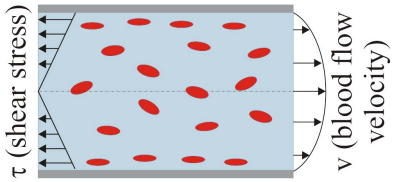

Fig. 3. Orientation and deformation of RBCs in a blood vessel.

for conductivity changes: one results from the increased volume in the systolic phase. The second one has its origin in blood flow velocity, because the red blood cells (RBCs) get oriented and deformed at higher flow rates, which increases the conductivity of blood.

If an AD occurs, the blood volume distribution as well as the blood flow profile changes compared to the healthy state, which of course leads to altered thoracic impedance characteristics. While the changes of the blood volume distribution can be easily modeled by adapting the geometry, a closer look at the flow-induced conductivity alteration of blood is necessary.

B. Flow-Induced Conductivity Changes of Blood

From experimental data, it has been shown that the electrical conductivity of flowing blood depends on the flow velocity [6]. The reason for this dependence is based on the orientation and deformation of the RBCs, which can be assumed as low-conducting ellipsoidal particles in a dilute suspension together with conducting plasma. At higher velocities, the shear stress increases and deforms the RBCs in the layer with the highest stress close to the vessel wall. RBCs are also aligned throughout the vessel as shown in Fig. 3. Both effects lead to a higher conductivity of blood.

The fraction of RBCs in the whole blood volume is approximately 45% and is called hematocrit H. Assuming that the conductivity of the RBCs is negligible compared to the plasma conductivity, the Maxwell–Fricke equation [7] for the conductivity of blood reads

$$\frac{\sigma_{\mathrm{bl}}}{\sigma_p} = \frac{1-H}{1+(C-1)H} \tag{1}$$

where σ_{bl} and σ_p are the conductivities of blood and the plasma, respectively, H is the hematocrit expressed as the volume fraction of RBCs relative to the total blood volume, and C is a factor that depends on the geometry and orientation of the RBCs.

Based on the formulations defined in [7], the blood conductivity σ_{bl} has been calculated analytically as a function of the spatial average velocity $\langle v \rangle$. Fig. 4 shows the relation for blood flow velocities as they occur in a healthy aorta (up to 300 cm/s) with an aortic radius of 1.1 cm.

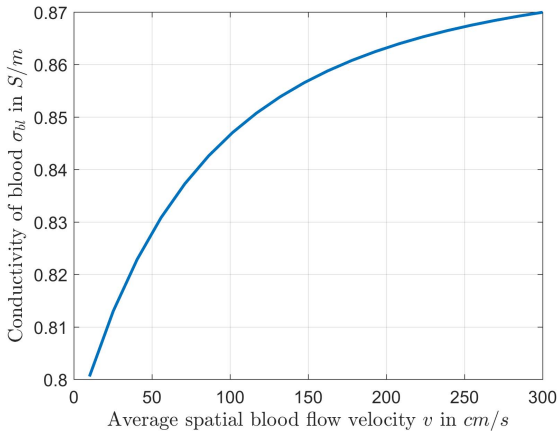

Fig. 4. Blood conductivity dependence on the blood flow velocity.

C. Simulation Model

A 3-D numerical simulation model is used to investigate the changes in the electric potential and, furthermore, the impedance changes on the thorax surface. The model has been set up in COMSOL Multiphysics software [8] for the underlying time-harmonic current flow problem. Since the duration of the cardiac pulse wave is much higher than the time period of the injecting current, simulations can be performed in the frequency domain.

Maxwell's equations to be solved describing a quasi-static electric field in the time-harmonic case are represented advantageously by the complex formalism

$$\nabla \times \mathbf{E} = \mathbf{0} \tag{2}$$

$$\nabla(\mathbf{J} + j\omega\mathbf{D}) = 0 \tag{3}$$

where $\mathbf{E}$ is the electric field intensity, $\mathbf{J}$ is the current density, $\mathbf{D}$ is the electric displacement, ω is the angular frequency, and j denotes the imaginary unit. Relation (2) allows introducing the electric scalar potential as

$$\mathbf{E} = -\nabla V. \tag{4}$$

Considering the constitutive laws

$$\mathbf{J} = \sigma\mathbf{E} \tag{5}$$

$$\mathbf{D} = \varepsilon\mathbf{E} \tag{6}$$

yields the partial differential equation

$$\nabla([\sigma + j\omega\varepsilon]\nabla V) = 0 \tag{7}$$

for V.

For the first investigations on impedance changes caused by an AD, the model consists of a simple geometry only, i.e., an elliptic cylinder for the thorax, a bent pipe for the aorta, and a parallel pipe to represent the false lumen in the dissected case as shown in Fig. 5.

The source electrodes are placed on the side of the thorax and inject an ac current with a magnitude of 5 mA and a

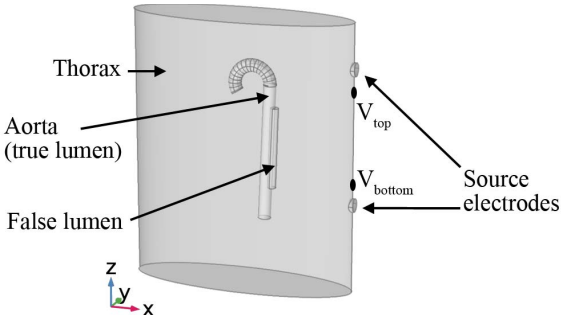

Fig. 5. Simulation model setup.

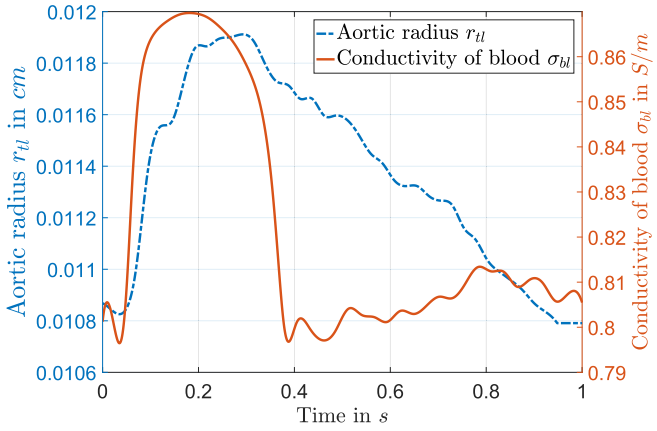

Fig. 6. Blood conductivity and aortic radius change over one cardiac cycle based on measurement data.

frequency of 100 kHz. The electric potential drop is evaluated between the source electrodes, which leads to the thoracic impedance

$$\underline{Z} = \frac{\underline{V}_{\text{top}} - \underline{V}_{\text{bottom}}}{\underline{I}}. \tag{8}$$

Surrounding material such as heart, lungs, and ribs are not considered directly, but a mean conductivity and permittivity are assigned to the thorax domain to provide a realistic value for the thoracic base impedance $|\underline{Z}_0|$ of about 40 Ω as reported in [9]. An appropriate conductivity and relative permittivity have been found with $\sigma_{\text{th}} = 0.08$ S/m and $\varepsilon_{r,\text{th}} = 8100$, respectively.

The conductivity of the aorta depends on the blood flow velocity as described in Section II-B and, therefore, changes with the cardiac pulse wave as well as the blood volume in the region of interest. Thus, measurement values of the blood flow velocity and the cross section of a healthy descending aorta provided in [10] are used as time-dependent input variables in the simulation model. Fig. 6 shows the variation of the analytically calculated conductivity and the aortic radius over a cardiac pulse wave based on these measurement data.

In case of an AD, blood starts to flow into the media layer and generates a false lumen there. It can be assumed that only a small amount of blood gets into the false lumen in each pulse cycle and that the blood flow is very low compared to that in the true lumen. Thus, the conductivity of blood in the false

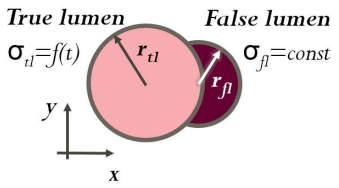

Fig. 7. Geometry and material properties in the dissected case.

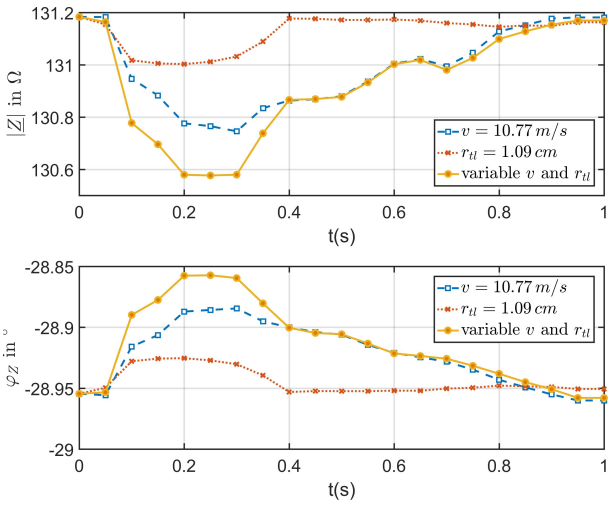

Fig. 8. Impact of blood volume and velocity on the thoracic impedance in a healthy aorta.

lumen is assumed to be constant over time with $\sigma_{\text{fl}} = 0.7$ S/m. In Fig. 7, a detailed view of the cross section of the descending aorta in the dissected state is shown.

III. Results

Before discussing the impedance changes due to an AD, the impact of the blood volume and the blood flow velocity changes on the thoracic impedance are shown for the healthy state (without considering a false lumen).

A. Impact of Blood Volume and Velocity on the Impedance Changes in a Healthy Aorta

By using the time-dependent variables for σ_{bl} and r_{tl} as shown in Fig. 6, the impedance change over one cardiac cycle has been simulated at 21 discrete time instants. To identify the impact of both input variables separately, one of the variables has been kept constant. In Fig. 8, it can be observed that the impact of the aortic radius change is much higher than the impact of the velocity change. Nevertheless, the velocity-based impedance changes should not be neglected since pathological changes in the aorta always strongly influence the blood flow velocity.

B. Impedance Changes in Case of an Aortic Dissection

In the dissected case, the false lumen pipe has been added with a constant conductivity $\sigma_{\text{fl}} = 0.7$ S/m and a radius $r_{\text{fl}} = 2$ cm. Also, the blood flow velocity in the true lumen has been reduced since the continuity equation for fluid flow

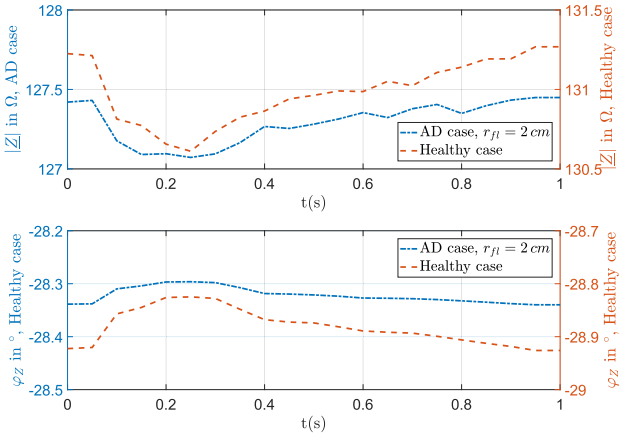

Fig. 9. Comparison between a healthy and an aortic dissected case.

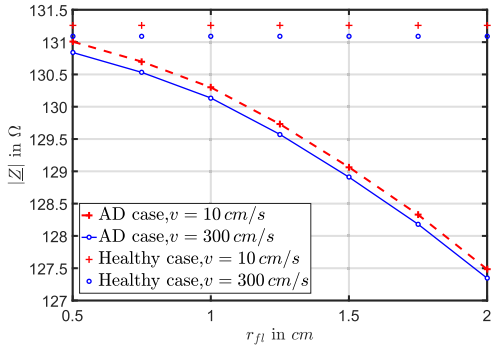

Fig. 10. Level of impedance change as a function of the false lumen size.

must hold and, additionally, the flow gets turbulent, which leads to lower velocity [11]. Thus, the velocity in the true lumen has been decreased by a factor of 0.6 compared to the healthy case.

In Fig. 9, it can be observed that the impedance decreases generally, which is explainable by the fact that the volume with higher conductivity (due to the additional blood in the false lumen) increases. On the other hand, the shape of the impedance over one cardiac cycle changes. At the time instant with the highest blood flow velocity ($t = 0.2$ s), the impedance alteration is much smaller than in the healthy case due to reduced velocity and, furthermore, reduced blood conductivity in the dissected case.

The impedance difference between the healthy and the aortic dissected case is 5 Ω in mean, which is well measurable in practice [12]. However, especially the unique impedance *profile* due to velocity changes appears promising regarding ascertain different aortic diseases, for example, aortic aneurysms, aortic stenoses, or ADs.

In Fig. 10, the relationship between the impedance change and the size of the false lumen is shown. It can be clearly observed that it will be difficult to identify ADs in early stages when the false lumen size is small. For example, if the cross section of the false lumen has the same size as one of the true lumens, which is the case at a radius $r_{\mathrm{fl}} = 1.38$ cm, the impedance difference is 2 Ω or 1.52% compared to the healthy case.

IV. Conclusion

A 3-D simulation model has been set up to investigate the possibilities and the limits for the identification of an AD by measuring the impedance changes on the thorax surface. The impedance differences between the healthy and the dissected state are in a practically measurable range. Nevertheless, since the thoracic base impedance of each patient may vary (due to the individual body and organ geometry), the absolute impedance difference cannot be evaluated without having prior information about the specific patient. In the best, but very unlikely case, a reference measurement from the past exists. Another possibility, which is very cumbersome and relatively inaccurate, is to simulate the base impedance by using detailed knowledge about the thoracic geometry from magnetic resonance or computed tomography images.

Therefore, a stronger focus will have to be put on recognizing characteristic *changes* in the impedance profile due to aortic diseases in future works.

Acknowledgment

This work was supported in part by the Graz University of Technology through the LEAD Project (2018–2021) "Mechanics, Modeling, and Simulation of Aortic Dissection."

References

[1] J. K. Lempel *et al.*, "Aortic arch dissection: A controversy of classification," *Radiology*, vol. 271, no. 3, pp. 848–855, Jun. 2014.
[2] J. Heuser, "Distributed under a CC-BY-SA-3.0 license," Wikimedia Commons, Tech. Rep., Apr. 2016.
[3] H. H. Woltjer, H. J. Bogaard, and P. M. de Vries, "The technique of impedance cardiography," *Eur. Heart J.*, vol. 18, no. 9, pp. 1396–1403, Sep. 1977.
[4] M. Cheney, D. Isaacson, and J. C. Newell, "Electrical impedance tomography," *SIAM Rev.*, vol. 41, no. 1, pp. 85–101, Aug. 1999.
[5] C. Gabriel, "The dielectric properties of biological tissue: I, literature survey," *Phys. Med. Biol.*, vol. 41, pp. 2231–2249, 1996.
[6] K. R. Visser, "Electric conductivity of stationary and flowing human blood at low frequencies," in *Proc. 21st Century Proc. Annu. Int. Eng. Med. Biol. Soc.*, Nov. 1989, pp. 1540–1542.
[7] A. E. Hoetink *et al.*, "On the flow dependency of the electrical conductivity of blood," *IEEE Trans. Biomed. Eng.*, vol. 51, no. 7, pp. 1251–1261, Jul. 2004.
[8] COMSOL AB, Stockholm, Sweden. *COMSOL Multiphysics Version 5.4*. Accessed: Nov. 4, 2018. [Online]. Available: http://www.comsol.com
[9] M. Ulbrich, P. Paluchowski, J. Mühlsteff, and S. Leonhardt, "High temporal resolution finite element simulations of the aorta for thoracic impedance cardiography," in *Proc. Comput. Cardiol.*, vol. 38, Sep. 2011, pp. 149–152.
[10] J. Alastruey, N. Xiao, H. Fok, T. Schaeffter, and C. A. Figueroa, "On the impact of modelling assumptions in multi-scale, subject-specific models of aortic haemodynamics," *J. Roy. Soc. Interface*, vol. 13, no. 119, Jun. 2016, Art. no. 20160073.
[11] R. L. Gaw, B. H. Cornish, and B. J. Thomas, "The electrical impedance of pulsatile blood flowing through rigid tubes: A theoretical investigation," *IEEE Trans. Biomed. Eng.*, vol. 55, no. 2, pp. 721–727, Feb. 2008.
[12] M. Snajdarova, S. Borik, and I. Cap, "Design of measurement device for impedance cardiography," in *Proc. 18th Int. Conf. Comput. Problems Elect. Eng. (CPEE)*, Kutná Hora, Czech Republic, Sep. 2017, pp. 1–4.